Eur. J. Biochem. **271**, 1789–1797 (2004) © FEBS 2004 doi:10.1111/j.1432-1033.2004.04096.x

Multiple-probe analysis of folding and unfolding pathways of human serum albumin

Evidence for a framework mechanism of folding

Manas Kumar Santra, Abhijit Banerjee, Shyam Sundar Krishnakumar, Obaidur Rahaman and Dulal Panda

School of Biosciences and Bioengineering, Indian Institute of Technology, Bombay, Mumbai, India

The changes in the far-UV CD signal, intrinsic tryptophan fluorescence and bilirubin absorbance showed that the guanidine hydrochloride (GdnHCl)-induced unfolding of a multidomain protein, human serum albumin (HSA), followed a two-state process. However, using environment sensitive Nile red fluorescence, the unfolding and folding pathways of HSA were found to follow a three-state process and an intermediate was detected in the range 0.25–1.5 M GdnHCl. The intermediate state displayed 45% higher fluorescence intensity than that of the native state. The increase in the Nile red fluorescence was found to be due to an increase in the quantum yield of the HSA-bound Nile red. Low concentrations of GdnHCl neither altered the binding affinity of Nile red to HSA nor induced the aggregation of HSA. In addition, the secondary structure of HSA was not perturbed during the first unfolding transition (< 1.5 M GdnHCl); however, the secondary structure was completely lost during the second transition. The data together showed that the half maximal loss of the tertiary structure occurred at a lower GdnHCl concentration than the loss of the secondary structure. Further kinetic studies of the refolding process of HSA using multiple spectroscopic techniques showed that the folding occurred in two phases, a burst phase followed by a slow phase. An intermediate with native-like secondary structure but only a partial tertiary structure was found to form in the burst phase of refolding. Then, the intermediate slowly folded into the native state. An analysis of the refolding data suggested that the folding of HSA could be best explained by the framework model.

Keywords: bilirubin; human serum albumin; framework model; Nile red; protein folding.

Human serum albumin (HSA), a major protein component of blood plasma, is the physiological carrier for a broad range of insoluble endogenous compounds like fatty acids, lysolecithin, bilirubin and bile salts [1,2]. It also binds to a wide variety of drugs [3–5]. It has three structurally similar α-helical domains I–III, which are further divided into subdomains A and B [6,7]. Recent evidences indicate the presence of one or more stable intermediates in the unfolding pathway of multidomain proteins suggesting that unfolding occurs through multiple steps [8,9]. Surprisingly, several studies reported that the denaturant-induced unfolding of the multidomain protein HSA occurred through a highly cooperative two-state process involving only the native and unfolded states [10–13]. For example, Tayyab *et al.* [10,11] found that the urea-induced unfolding of HSA apparently occurred in a single, concerted step with no intermediate formation. Further, Muzammil *et al.* [12] found that guanidine hydrochloride (GdnHCl)-induced unfolding occurred in a single step. In addition, a recent analysis involving multiple probes and the changes in spatial distances between these probes have shown that GdnHCl-induced unfolding of HSA occurred through an incremental loss of structure but no stable intermediate state was identified in the unfolding process [13]. However, Flora *et al.* [14] reported that unfolding of HSA by GdnHCl occurred in multiple steps, with at least one intermediate. Thus, the presence of an intermediate state in the unfolding pathway of HSA remains controversial.

In many proteins, although an intermediate forms during the unfolding process, the intermediate is often not detected due to the lack of an appropriate probe. It is believed that the detection of an intermediate under equilibrium conditions helps in understanding the mechanisms of protein unfolding and folding and that the folding intermediates greatly assist in narrowing the search for the native state by increasing native-like interactions [5–18]. However, often the intermediates are trapped kinetically in the folding pathway by non-native interactions that significantly reduce the folding rate. These intermediates are comprised of misfolded or randomly collapsed species [17,19–22]. The partially folded intermediates that are formed under various folding conditions may have different secondary structures and compactness depending on the protein and the experimental conditions. Further, the intermediate states are not necessarily close either to the native or the unfolded state [23]. These findings suggest that protein folding occurs through a diverse array of mechanisms [16,24,25].

Three models, namely the framework model, the hydrophobic collapse model and the nucleation model are frequently used to describe the mechanism of protein

Correspondence to D. Panda, School of Biosciences and Bioengineering, Indian Institute of Technology, Bombay, Mumbai 400 076, India. Fax: + 91 22 2572 3480, Tel.: + 91 22 2576 7838, E-mail: panda@iitb.ac.in

Abbreviations: HSA, human serum albumin; GdnHCl, guanidine hydrochloride; ANS, 1-anilinonaphthalene-8-sulfonic acid.

(Received 19 January 2004, revised 3 March 2004, accepted 18 March 2004)

folding [24–32]. The framework model involves the formation of the tertiary structures through a hierarchical assembly of the local elements of the secondary structures [24,25,29–31,33]. The framework model has been extended to include the mechanism where some extent of the tertiary structures is also formed along with the secondary structure. The hydrophobic collapse model, involves the formation of a loose hydrophobic core followed by the development of secondary structural elements resulting in the formation of the tightly packed native structure [26,29]. According to the nucleation model, the folding process of a protein starts with the formation of a rate-limiting configuration by native-like contacts of neighbouring residues, which then nucleates into the native structures [27–29]. In the nucleation model, the tight packing occurs rapidly without the formation of an intermediate, whereas for both the hydrophobic collapse and framework models, the tight packing occurs only after the formation of an intermediate state.

The folding pathway of HSA could be a complex process because each domain could fold independently and the inter-domain interactions could regulate the overall folding process. However, very little is known about the folding mechanism of HSA. In this report, multiple probes including bilirubin absorbance, tryptophan fluorescence, Nile red fluorescence and far-UV CD spectroscopy were used to identify and characterize the transitions that occurred during the folding–unfolding of HSA. An intermediate state was identified in both the unfolding and folding pathways of HSA and we obtained evidence suggesting that the folding of HSA follows the framework model.

Experimental procedures

Materials

HSA, fraction V, essentially fatty acid free was purchased from Calbiochem. According to the manufacturer the purity level of HSA is ≥98%. We also confirmed the purity level of HSA by Coomassie blue staining of SDS/PAGE (data not shown). GdnHCl was obtained from Aldrich Chemical Co. Dicumarol, Sephadex G-25 and bilirubin were from Sigma Chemical Co. Nile red and 1-anilinonaphthalene-8-sulfonic acid (ANS) were from Molecular Probes. All other chemicals used in this study were of analytical grade.

Binding of Nile red to HSA

Free Nile red in aqueous solution has negligible fluorescence. Upon binding to HSA, the fluorescence intensity at 615 nm increased severalfold. Nile red has limited solubility in aqueous buffer. Therefore, low concentrations of Nile red were used to determine its affinity to HSA. HSA (1 μM) was incubated with different concentrations (0.2–0.7 μM) of Nile red in 25 mM phosphate buffer (pH 7) at 25 °C for 30 min. The dissociation constant of HSA and Nile red interaction was determined using Eqn (1):

$$\Delta F = \Delta F_{max} - K_d(\Delta F/[L]) \quad (1)$$

where ΔF_{max} is the maximum fluorescence when all the binding sites are saturated with Nile red, $[L]$ is the free ligand concentration, ΔF is the change in fluorescence when Nile red and HSA were in equilibrium and K_d is the dissociation constant. ΔF_{max} was determined using a reverse titration wherein a fixed concentration of Nile red (0.5 μM) was titrated with increasing amount of HSA in 25 mM phosphate buffer pH 7 at 25 °C for 30 min. ΔF_{max} was determined by plotting $1/(F–F_0)$ vs. 1/HSA and extrapolating 1/HSA to zero. Here, F_0 and F were the observed fluorescence intensities of Nile red in the absence and presence of different concentrations of HSA, respectively. Fluorescence measurements were performed using a JASCO FP-6500 fluorescence spectrophotometer (Jasco, Tokyo, Japan) at 25 °C equipped with a constant temperature water-circulating bath. The excitation and emission band passes were set at 5 nm and 10 nm, respectively. A quartz cell of 0.3 cm path length was used for all experiments if not stated otherwise.

Unfolding of HSA probed by Nile red fluorescence

HSA (2 μM) in 25 mM phosphate buffer pH 7 was incubated with different concentrations of GdnHCl (0.25–7 M) at 25 °C for 30 min. Nile red (0.5 μM) was then added to the reaction mixtures and incubated for an additional 30 min before spectral measurements. The emission spectra were collected over the range of 575–675 nm using 550 nm as an excitation wavelength.

Steady-state unfolding of HSA probed by intrinsic tryptophan fluorescence

HSA (2 μM) in 25 mM phosphate buffer pH 7 was denatured by different concentrations of GdnHCl (0.25–7 M) at 25 °C for 1 h. The emission spectra were collected over the range of 310–400 nm using 295 nm as an excitation wavelength.

Unfolding of HSA in the presence of bilirubin

The binding of bilirubin to HSA increases the ligand's absorbance at 475 nm. HSA (10 μM) was denatured by different concentrations of GdnHCl (0.5–7 M) for 30 min at 25 °C. Then, 10 μM of bilirubin was added to individual samples and incubated for 30 min under identical conditions before taking the absorbance at 475 nm. Absorbance measurements were performed using a JASCO V-530 UV-visible spectrophotometer.

Unfolding of HSA was probed by monitoring the change in the secondary structure

HSA (5 μM) in 25 mM phosphate buffer was incubated with different concentrations of GdnHCl at 25 °C for 30 min. The far-UV (200–260 nm) CD spectra were recorded at 25 °C using a JASCO spectropolarimeter (model J-810) equipped with a JASCO PTC 423S Peltier temperature control system. A quartz cuvette of 1-mm path length was used for all far-UV CD measurements performed in this study. Spectra were collected with a scan speed of 200 nm·min^{-1} and a response time of 1 s. Each spectrum was the average of five scans. The CD data were analysed using a JASCO software package.

Refolding studies by monitoring Nile red fluorescence

HSA (100 μM) was incubated with 6 M GdnHCl for 30 min at 25 °C in 25 mM sodium phosphate buffer pH 7. Under these conditions, HSA was found to be fully unfolded as judged by Nile red fluorescence, tryptophan fluorescence and far-UV CD spectroscopy. The unfolded sample was diluted 50 times in phosphate buffer to adjust the final concentration of HSA to 2 μM. At desired time point, Nile red was added to an aliquot of the diluted unfolded sample and incubated for 2 min. The binding of Nile red to HSA was found to be complete within 2 min. After 2 min of incubation at 25 °C, Nile red fluorescence was monitored as described previously. The fraction refolded was calculated by using the following equation:

$$F_r = 1 - \frac{F_N - F}{F_N - F_D} \quad (2)$$

where F_r is the fraction refolded, F is the observed Nile red fluorescence intensity at different time intervals, F_N is the fluorescence intensity of the native HSA–Nile red complex and F_D is the fluorescence intensity of HSA–Nile red complex in the presence of 6 M GdnHCl.

Refolding studies by monitoring tryptophan fluorescence

As described for Nile red, HSA (100 μM) was first unfolded by incubating with 6 M GdnHCl. Then, the unfolded HSA was diluted 50 times in phosphate buffer and the kinetics of refolding were followed by monitoring tryptophan fluorescence. The excitation and emission wavelengths were 295 nm and 340 nm, respectively. The fraction of refolding at different times was calculated using Eqn (2).

Ligand binding properties of refolded HSA

HSA was completely unfolded by incubating with 6 M GdnHCl for 1 h. The denaturant was removed by exhaustive dialysis at 4 °C against 25 mM phosphate buffer pH 7. Native or refolded HSA (3 μM) was incubated with different concentrations (0–50 μM) of dicumarol for 30 min at 25 °C in 25 mM phosphate buffer pH 7. The binding of dicumarol to the native and refolded HSA was determined by monitoring the decrease in the tryptophan fluorescence of HSA. Native or refolded HSA (3 μM) was incubated with different concentrations (10–50 μM) of ANS for 30 min at 25 °C. The binding of ANS to the native and refolded HSA was measured by measuring ANS fluorescence intensity at 475 nm using 360 nm as an excitation wavelength. Bilirubin (5 μM) was incubated with 5 μM of the native or refolded HSA for 30 min at 25 °C and the binding of bilirubin to the native and refolded HSA was determined by measuring the bilirubin absorbance at 475 nm.

Light scattering assay

The light scattering of 10 μM HSA was monitored for 15 min in the absence and presence of different concentrations (0.25 M, 0.5 M and 1 M) of GdnHCl. The excitation and emission wavelengths were set to 400 nm with excitation and emission band pass of 3 nm and 5 nm, respectively.

Calculation of D_m values from equilibrium unfolding

Several experiments demonstrated that the free energy (ΔG_{U-F}) of unfolded proteins at different denaturant concentrations [D] has a linear relationship with the denaturant concentration [34]:

$$\Delta G_{U-F}{}^{D} = \Delta G_{U-F}{}^{H_2O} - m[D] \quad (3)$$

where m is the slope of the transition, $\Delta G_{U-F}{}^{H_2O}$ is the free energy of unfolding in the absence of denaturant. The fluorescence intensity (F) of a protein at equilibrium with different concentrations of denaturant [D] can be expressed as:

$$F = [(\alpha_F + \beta_F[D]) + (\alpha_U + \beta_U[D]) \times \exp\{m([D] - D_m)/RT\}]/ [1 + \exp\{m([D] - D_m)/RT\}] \quad (4)$$

where α_F and α_U are the intercepts and β_F and β_U are the slopes of the baselines of the equilibrium fluorescence (F) at low and high denaturant concentrations, respectively. D_m is the denaturant concentration at which 50% of the protein is unfolded. R is the universal gas constant and T is the absolute temperature. The data were fitted to this equation using the linear least-squares method to obtain the best-fitted values of m and D_m. The curve fittings were performed using MICROSOFT ORIGIN software.

Calculation of the rate constants from the kinetics of refolding

HSA was found to follow two phases of refolding, a burst phase and a slow phase. The burst phase occurred within the dead-time of the experiment. The rate constant of the burst phase could not be estimated as there were not sufficient data points in the burst phase. The rate of the slow phase was calculated using both tryptophan and Nile red fluorescence. The fluorescence intensity of tryptophan or Nile red was related to the rate of the refolding reaction by Eqn (5):

$$I = I_U + (1 - e^{-kT}) \times (I_F - I_U) \quad (5)$$

where, I_u and I_f were the fluorescence intensities of the unfolded and folded proteins, respectively, T is the absolute temperature and k is the rate constant of the refolding reaction. Eqn (5) was fitted to the kinetic data to obtain the best-fitted values of k.

Results

Unfolding of HSA was monitored by the Nile red fluorescence

Free Nile red in aqueous solution had negligible fluorescence but its fluorescence increased 18-fold upon the addition of 2 μM HSA (Fig. 1A). The equilibrium unfolding pathways of HSA were investigated using environment-sensitive Nile red fluorescence. The fluorescence intensity of the HAS-bound Nile red varied in a complex fashion with increasing concentration of GdnHCl (Fig. 1A). For example, the fluorescence intensity increased in the presence of 0.25 M GdnHCl and decreased at higher concentrations of GdnHCl (Fig. 1A). The changes in fluorescence intensity at

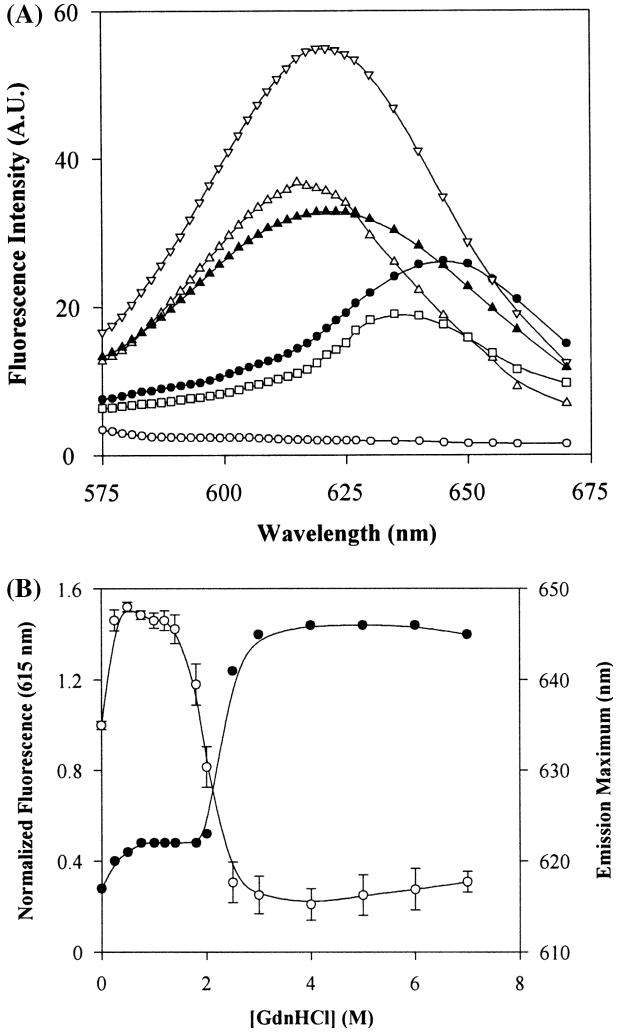

Fig. 1. The fluorescence spectrum of HSA-bound Nile red in the absence and presence of GdnHCl. (A) Absence of GdnHCl (△), with 0.25 M (▽), 2 M (▲), 4 M (□) and 7 M GdnHCl (●). Free Nile red (0.5 μM) fluorescence spectrum in the absence of HSA was denoted by (○). The fluorescence intensities of HSA-bound Nile red at 615 nm (○) and emission maximum (●) are plotted against GdnHCl concentration in (B). All spectra were corrected by subtracting the appropriate blank (spectra containing 0.5 μM Nile red in the presence of different concentrations of GdnHCl in the absence of HSA) from the original spectra.

615 nm of the HSA–Nile red complex along with the changes in the wavelength of emission maximum with increasing concentration of GdnHCl are shown in Fig. 1B. The fluorescence intensity of HSA–Nile red complex increased by ≈44% in the presence of 0.25 M GdnHCl and the intensity did not change until 1.5 M GdnHCl. The fluorescence intensity of free Nile red (in the absence of HSA) was increased only by 6% in the presence of 0.25 M GdnHCl showing that the increased fluorescence intensity of the HSA–Nile red complex in the presence of 0.25 M GdnHCl was not due to an increase in the quantum yield of the unbound Nile red. Further, there was a minimal increase (3 nm) in the emission maximum of HSA–Nile red complex fluorescence up to 1.5 M GdnHCl (Fig. 1B). Beyond 1.5 M GdnHCl, the fluorescence intensity of bound Nile red decreased sharply with increasing concentration of GdnHCl accompanied by a large red shift (26 nm) of the wavelength of emission maximum (Fig. 1B). The unfolding of HSA appeared to occur through two transitions with the formation of an intermediate (Fig. 1B). The first transition occurred at low concentrations of GdnHCl (< 1.5 M) that increased the exposure of the hydrophobic surface around Nile red binding site on HSA and the second unfolding transition destroyed most of the hydrophobic surfaces of the protein. The calculated value for the mid-point of unfolding transition (D_m) was 2.0 ± 0.01 M GdnHCl.

The enhanced Nile red fluorescence in the presence of low concentrations of GdnHCl may be due to either an increase in the Nile red binding to HSA or due to an increase in the quantum yield of the HSA-bound Nile red. To discern the possibilities, the dissociation constants of Nile red binding to HSA were determined under mild denaturation conditions. The dissociation constants (K_d) of Nile red and HSA interaction were found to be 0.39 ± 0.03 μM in the absence of GdnHCl, 0.42 ± 0.04 μM in the presence of 1 M GdnHCl and 1.72 ± 0.32 μM in the presence of 2.2 M GdnHCl. The data indicated that the observed increase in Nile red fluorescence at low concentrations of GdnHCl was not due to an increase of Nile red binding to HSA. Further, the increase in Nile red (0.5 μM) fluorescence was measured in the presence of low (2 μM) and high (50 μM) concentrations of HSA. In the presence of 50 μM HSA, the free Nile red concentration would be negligible since the K_d of the Nile red and HSA interaction was 0.39 ± 0.03 μM. GdnHCl (1 M) increased the bound Nile red fluorescence 44.8 ± 2.9% in the presence of 2 μM HSA and 44.7 ± 2.0% in the presence of 50 μM HSA compared to control (in the absence of GdnHCl). The data suggested that the increase in Nile red fluorescence in the presence of 1 M GdnHCl was due to an increase in the quantum yield of the HSA-bound Nile red.

We also investigated whether low concentrations of GdnHCl (0.25 M, 0.5 M and 1 M) could induce the aggregation of HSA by using a standard light scattering technique [35,36]. Low concentrations of GdnHCl did not increase the light scattering signal at 400 nm compared to the control HSA (in the absence of GdnHCl) signal suggesting that low concentrations of GdnHCl did not induce aggregation of HSA (data not shown).

Steady-state unfolding of HSA was probed by tryptophan fluorescence and bilirubin binding

There was a minimal (≈ 8%) increase in the tryptophan fluorescence of HSA in the presence of low concentrations of GdnHCl (0.6 M–1.4 M) (Fig. 2). However, tryptophan fluorescence decreased sharply beyond 1.6 M GdnHCl indicating that the unfolding process is cooperative. The limiting fluorescence intensity was reached at 4 M GdnHCl. The tryptophan fluorescence intensity changes were fitted in a two state transition model that yielded a D_m value of 2.0 ± 0.01 M.

Bilirubin binds to HSA at drug binding site I of the domain II [37,38]. As shown in Fig. 2, bilirubin binding was minimally altered at low concentrations (< 2 M) of GdnHCl but the binding of bilirubin to HSA decreased

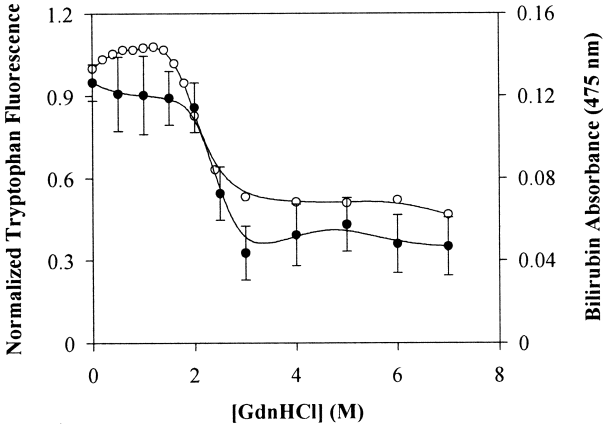

Fig. 2. GdnHCl-induced unfolding of HSA was probed by the intrinsic tryptophan fluorescence (○) and bilirubin binding (●). Intrinsic tryptophan fluorescence intensities at 340 nm were recorded from the emission spectra and the fluorescence intensities were normalized against the tryptophan fluorescence intensity of the native HSA. The interaction of bilirubin with HSA was monitored by the change in absorbance at 475 nm.

sharply beyond 2 M GdnHCl. The nonlinear regression analysis of the data in a two state transition model produced a D_m value of 2.5 ± 0.1 M.

Secondary structural changes during equilibrium unfolding and refolding of HSA monitored by far-UV CD

The far-UV CD spectra was not perturbed by ≈1.5 M GdnHCl indicating that the secondary structure of HSA was not detectably changed (Fig. 3A). However, higher concentrations of GdnHCl perturbed the far-UV CD spectra of HSA in a concentration-dependent fashion (Fig. 3A). The changes in CD at 220 nm with increasing GdnHCl concentration are shown in Fig. 3B. The D_m value was calculated to be 2.8 ± 0.1 M and the complete loss of secondary structure occurred at 5 M GdnHCl (Fig. 3B). The refolding isotherm was found to be similar to the unfolding isotherm and the D_m was estimated to be 2.8 ± 0.2 M (Fig. 3B). The data indicated that HSA undergoes reversible folding process.

Kinetics of HSA refolding was probed by tryptophan fluorescence, Nile red fluorescence and far-UV CD spectroscopy

Tryptophan fluorescence has been used extensively to monitor the recovery of tertiary structure during the refolding processes of several proteins [39,40]. We also examined the refolding kinetics of HSA by monitoring the intrinsic tryptophan fluorescence spectra of HSA at different time points (Fig. 4A). The kinetics of refolding appeared to follow two phases, a burst phase and a slow phase (Fig. 4B). During the burst phase, 50% recovery of the tryptophan fluorescence occurred at 30 s of refolding. However, the complete recovery of the tryptophan fluorescence took almost 2 h indicating that the remaining part of the folding occurred through a slow phase. The rate constant of the burst phase of the refolding step could not

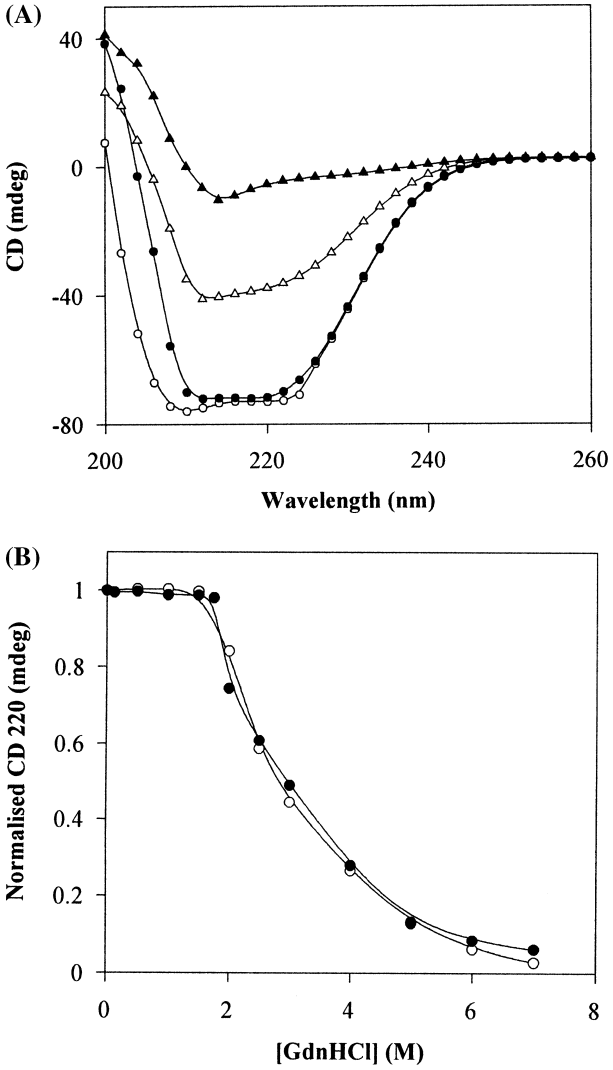

Fig. 3. The effect of GdnHCl on the far-UV CD spectra of HSA. (A) CD spectra of HSA in the absence (○) and presence of 1.5 M (●), 2.5 M (△) and 6 M (▲) GdnHCl. (B) The 220 nm CD signals at different concentrations of GdnHCl were normalized with respect to the control signal (in the absence of GdnHCl) and plotted against GdnHCl concentrations (B) during unfolding (○) and refolding of HSA (●). HSA (2 μM) in the absence of GdnHCl was used as the control.

be estimated due to the lack of sufficient data points. The apparent rate of the slow phase was estimated to be 0.016 ± 0.002 min^{-1} by fitting the data in Eqn (5). The fluorescence intensity of the native HSA did not change during the experimental duration.

The kinetics of refolding was also measured by the recovery of the Nile red fluorescence as described in Experimental procedures. The kinetics of refolding of HSA appeared to be bi-phasic (Fig. 5). The burst phase of refolding occurred rapidly with 71% of refolding happened within the first 2 min of dilution in GdnHCl-free buffer. In the slow phase of refolding almost 90% of folding was observed by 10 min of refolding. The apparent rate constant of the slow phase was estimated to be 0.12 ± 0.02 min^{-1} by fitting the data points of the slow phase in Eqn (5).

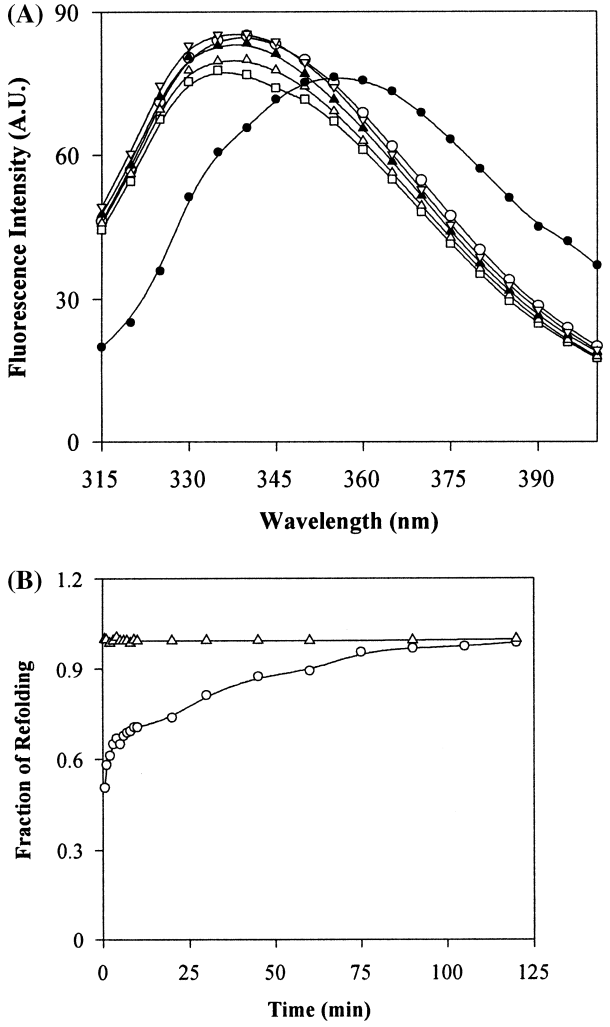

Fig. 4. Kinetics of HSA refolding monitored by tryptophan fluorescence. (A) Tryptophan spectra of 2 μM HSA in the absence (○) and presence of 6 M (●) GdnHCl. The spectra defined by the symbols □, △, ▲ and (▽) represent 30 s, 45 min, 90 min and 120 min of refolding, respectively. (B) Fraction of tryptophan fluorescence recovery (○) at different time points. The fluorescence (△) of the native HSA (2 μM) did not change during the duration of the experiment. The extent of refolding was calculated as described in Experimental procedures.

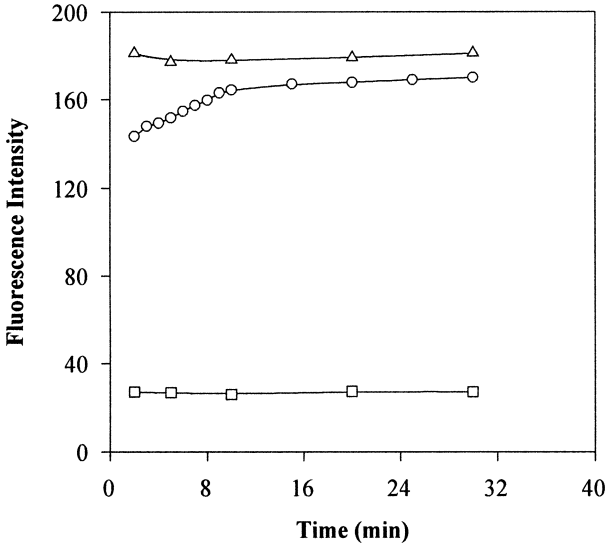

Fig. 5. Kinetics of HSA refolding measured by Nile red fluorescence. The refolding kinetics (○) of HSA was measured by the fluorescence intensity of the HSA–Nile red complex at 615 nm. The fluorescence intensities of the native HSA–Nile red complex (△) and the completely unfolded HSA–Nile red complex (□) did not change during the experiment.

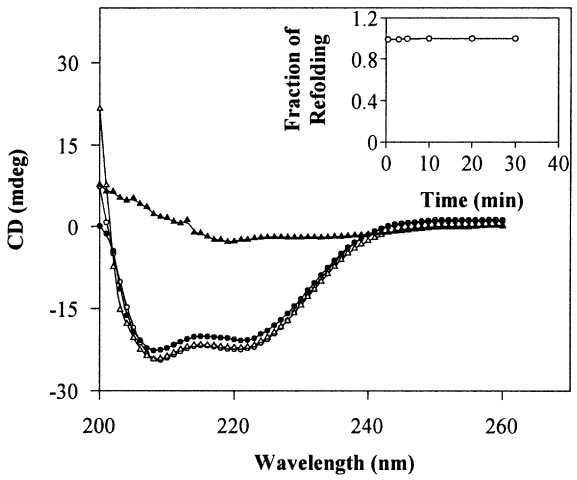

Fig. 6. Kinetics of secondary structure formation of HSA during refolding. The recovery of secondary structure was monitored by monitoring far UV-CD spectra at different time points. The figure shows the spectra taken at 30 s (●) and 20 min (△) after dilution. The far UV-CD spectra of 2 μM native HSA (○) in the absence of GdnHCl and 2 μM unfolded HSA (▲) in the presence of 6 M GdnHCl are also shown for comparison. The fractional recovery of the 220 nm CD signal is shown (inset).

Finally, the refolding kinetics of HSA was examined by monitoring the increase of far-UV CD signals with time (Fig. 6). Almost complete (> 98%) recovery of the 220 nm CD signal was observed within the first 30 s of refolding (Fig. 6, inset). Thus, the formation of the secondary structure of HSA occurred at much faster rate than the formation of the tertiary structure as probed by the recovery of tryptophan fluorescence and Nile red fluorescence.

Refolding of HSA in the presence of different concentrations of GdnHCl probed by Nile red fluorescence

Using Nile red fluorescence, we detected an intermediate state in the unfolding pathway of HSA (Fig. 1A). To verify that the intermediate state was indeed a part of the folding pathway, and not an experimental artefact, refolding kinetics of HSA in the presence of different concentrations of GdnHCl were performed (Fig. 7). After unfolding HSA in 6 M GdnHCl, refolding was initiated by appropriate dilution of the unfolded protein in phosphate buffer containing varying concentrations of GdnHCl and the recovery of the Nile red fluorescence was monitored. During refolding process, the fluorescence intensity of Nile red

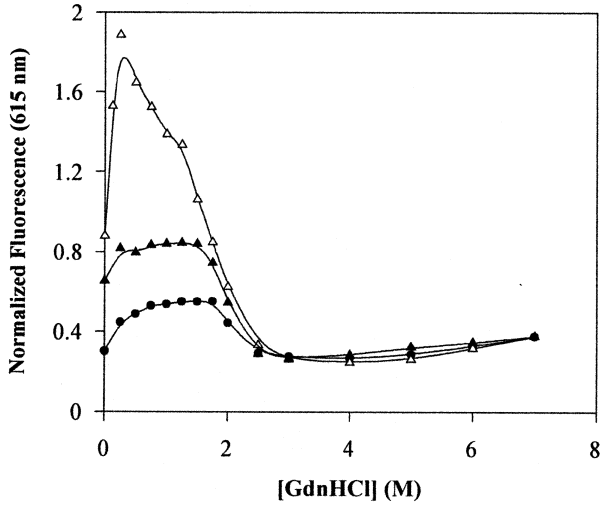

Fig. 7. Equilibrium refolding of HSA in the presence of different concentrations of GdnHCl. The recovery of the Nile red fluorescence at 1 h (●), 12 h (▲) and 24 h (△) was monitored as described in the Experimental procedures.

changed in a manner that was observed during the unfolding process of HSA indicating that an intermediate was also formed in the folding pathway. The fluorescence intensity of the intermediate state remained constant for a narrow GdnHCl concentration range for the longer incubation time. The estimated D_m values were 2.2 ± 0.1 M, 2 ± 0.01 M and 1.5 ± 0.1 M for 1 h, 12 h and 24 h of refolding, respectively. The results together indicated that the stability of the intermediate state decreased with increasing incubation time.

Ligand binding properties of the refolded HSA

HSA was completely unfolded by incubating with 6 M GdnHCl for 1 h. After removal of GdnHCl, the ligand binding ability of the refolded HSA was compared with that of the native HSA. Bilirubin, dicumarol and ANS were found to bind to the native and refolded HSA similarly showing that the refolded HSA regained its ligand binding ability completely (data not shown). In addition, tryptophan fluorescence spectra and far-UV CD spectra of the native HSA and refolded HSA were found to be identical. The results together showed that no misfolding occurred during the refolding process and that the unfolding of HSA was completely reversible. Previous studies also showed that the GdnHCl-induced unfolding of HSA was reversible [13,41].

Discussion

The highly cooperative changes in tryptophan fluorescence, bilirubin absorbance and the far-UV CD spectra suggested that the unfolding process of HSA involves only a native and an unfolded state, i.e. the reaction follows a two-state process (Figs 2 and 3). However, the initial increase and the subsequent decrease of Nile red fluorescence at low and high concentrations of GdnHCl indicated that at least one relatively stable intermediate was formed during the unfolding of HSA. Similar to unfolding, at least one intermediate was detected in the folding profile of HSA using Nile red fluorescence. The stability of the equilibrium refolding intermediate was found to decrease in the presence of moderate concentrations of GdnHCl with increasing incubation time. The Nile red fluorescence of the intermediate was found to increase with incubation time suggesting that the nature of the intermediate changed after prolonged incubation with GdnHCl (Fig. 7). The increase in the Nile red fluorescence of the intermediate with incubation time could be due to an increase in the hydrophobic environment surrounding the probe. The multidomain structure of HSA could be the structural basis of the formation of the equilibrium intermediate, as the domains may unfold and fold independently.

Despite overlap in the effective GdnHCl concentrations needed to unfold HSA, the GdnHCl-induced unfolding of HSA occurred in a stepwise fashion. The calculated D_m values for GdnHCl-induced unfolding of HSA probed by tryptophan fluorescence, Nile red fluorescence and far-UV CD were 2.0 ± 0.01 M, 2.0 ± 0.01 M and 2.8 ± 0.2 M, respectively. Thus, the tertiary structure was lost at a lower concentration of GdnHCl compared to the secondary structure suggesting that the secondary structure of HSA is more stable than its tertiary structure. The first unfolding transition that occurred in the presence of 0.25 M GdnHCl was accompanied by a significant increase (≈45%) in the fluorescence intensity of the HSA–Nile red complex (Fig. 1B). The fluorescence intensity of free Nile red was increased only 6% by the low concentration of GdnHCl showing that the enhanced fluorescence of the HSA–Nile red complex was not caused by an increase of the quantum yield of the free Nile red. Interestingly, the dissociation constant of HSA and Nile red interaction did not change in the presence of low concentrations of GdnHCl. Further, the fluorescence intensity of the fully bound Nile red (in the presence of 100-fold excess HSA) also increased by ≈45% in the presence of 1 M GdnHCl indicating that the increased fluorescence intensity at low concentration of GdnHCl was due mainly to an increase in the quantum yield of the Nile red and not due to the generation of new Nile red binding sites. It appears that low concentrations of GdnHCl induce rearrangement of hydrophobic surfaces around Nile red binding site on HSA in a way that the probe experiences more hydrophobic environment than the native conformation of HSA, which results in an increase in the quantum yield of the bound probe. The CD analysis showed that no significant alteration in the secondary structure occurred during the first unfolding transition, indicating that the first transition involves local tertiary structure rearrangement, with no detectable change in secondary structure. Low concentration (< 1.5 M) of GdnHCl minimally altered the intrinsic tryptophan fluorescence of HSA. Therefore, the intermediate state that was detected by the Nile red fluorescence has native-like secondary structure and tertiary topology but it contained 45% more exposed hydrophobic surface than the native HSA.

Upon removal of GdnHCl, HSA gained its tryptophan fluorescence, secondary structure and ligand binding abilities indicating that HSA undergoes reversible folding and unfolding processes (Figs 4–6 [13]). However, the equilibrium refolding profile of HSA monitored by the Nile red

fluorescence did not match well with that of the unfolding profile in the presence of GdnHCl (Fig. 1B and Fig. 7). The disparity between the unfolding and refolding profiles of HSA suggested that the intermediates formed during the folding and unfolding processes in the presence of GdnHCl were not identical. Some misfolded off-pathway intermediates could also be formed when the unfolded HSA was incubated with moderate concentrations of GdnHCl for longer durations (Fig. 7).

The refolding process was initiated by diluting the unfolded HSA in GdnHCl-free buffer. The far-UV CD spectrum of refolded HSA was indistinguishable from that of the native protein within 30 s of dilution while the protein recovered only 50% of its tryptophan fluorescence at 30 s (Figs 4 and 6). The data suggested that the folding pathway of HSA involved at least one intermediate (I), which contained native-like secondary structures but only a partial tertiary structure. The pattern of the recovery of the tryptophan fluorescence intensity indicated that the folding of HSA occurred in a biphasic manner, a burst phase followed by a slow phase. The slow phase may be due to some kinetically unfavourable structural rearrangements of the protein. Like tryptophan fluorescence, the Nile red fluorescence intensity also showed a similar kinetic pattern of HSA refolding; 71% of the Nile red fluorescence was recovered within 2 min of refolding while the recovery of the remaining fluorescence was a relatively slow process (Fig. 5). The initial burst phase was not detectable using Nile red fluorescence because the kinetics of Nile red binding to HSA was a much slower process than the burst phase of the refolding. Although, the estimated values of the apparent rate constants of the slow phase obtained from tryptophan and Nile red fluorescence differed from each other, both probes showed a similar overall pattern of refolding kinetics of HSA, a burst phase followed by a slow phase of refolding. The change in the fluorescence intensity of a probe depends on the change in its surroundings. The discrepancy in the rate constants of the slow phase may be due to a difference in the rates of folding of the local environment of the probes. Taken together, the results of the kinetic studies suggested that an intermediate was formed at the burst phase of refolding, which contained most of the secondary structures of the native state but did not have native-like rigid side chain packing and subsequently, the intermediate refolded to the native state (N) through a slow phase. Therefore, the refolding scheme of HSA can be described as:

$$U \xrightarrow{\text{Burst}} I \xrightarrow{\text{Slow}} N$$

The secondary structure of HSA was completely formed within 30 s of refolding whereas only 50% of the tryptophan fluorescence was recovered within that time suggesting that the secondary structure of HSA was completed prior to the completion of tertiary structure. The data suggested that the folding of HSA follows a framework model wherein the formation of the tertiary structure occurs through a hierarchical assembly of the local elements of the secondary structures [29–31]. However, we cannot rule out the possibility that a native-like tertiary topology started to form at a very early stage of folding as 50% of the tryptophan fluorescence and 71% of Nile red fluorescence were recovered by 30 s and 2 min of refolding, respectively, supporting a hierarchical framework-like model for the folding of HSA. The hierarchical framework model is an extended version of the framework model where some extent of the tertiary structures is also formed along with the secondary structure [31,32]. The subtle difference between the framework model and the hierarchical framework-like model makes it very difficult to distinguish between these models because a native-like tertiary backbone was also found to exist for several proteins at very early stages of folding although the formation of the secondary structure preceded the formation of the tertiary structure [30,42–44].

Acknowledgements

We thank I.N.N. Namboothiri, D. Dasgupta and P. Ghosh for critical reading of the manuscript. This work was supported by a grant to D. P. from the Department of Science and Technology, Government of India and a Council of Scientific and Industrial Research fellowship to M. K. S. from the Government of India.

References

1. Berde, C.B., Hudson, B.S., Simoni, R.D. & Sklar, L.A. (1979) Human serum albumin. Spectroscopic studies of binding and proximity relationships for fatty acids and bilirubin. *J. Biol. Chem.* **254**, 391–400.
2. Peters, T. (1985) Serum albumin. *Adv. Protein Chem.* **37**, 161–245.
3. Sjoholm, I., Ekman, B., Kober, A., Ljungstedt-Pahlman, I., Seiving, B. & Sjodin, T. (1979) Binding of drugs to human serum albumin. XI. The specificity of three binding sites as studied with albumin immobilized in microparticles. *Mol. Pharmacol.* **16**, 767–777.
4. Kragh-Hansen, U. (1988) Evidence for a large and flexible region of human serum albumin possessing high affinity binding sites for salicylate, warfarin, and other ligands. *Mol. Pharmacol.* **34**, 160–171.
5. Nerli, B., Romanini, D. & Picó, G. (1997) Structural specificity requirements in the binding of beta lactam antibiotics to human serum albumin. *Chem. Biol. Interacts* **104**, 179–202.
6. He, X.M. & Carter, D.C. (1992) Atomic structure and chemistry of human serum albumin. *Nature* **358**, 209–215.
7. Carter, D.C. & Ho, J.X. (1994) Structure of serum albumin. *Adv. Protein Chem.* **45**, 152–203.
8. Das, B.K., Bhattacharyya, T. & Roy, S. (1995) Characterization of a urea induced molten globule intermediate state of glutaminyl-tRNA synthetase from *Escherichia coli*. *Biochemistry* **34**, 5242–5247.
9. Jansens, A., van Duijn, E. & Braakman, I. (2002) Coordinated nonvectorial folding in a newly synthesized multidomain protein. *Science* **298**, 2401–2403.
10. Muzammil, S., Kumar, Y. & Tayyab, S. (1999) Molten globule-like state of human serum albumin at low pH. *Eur. J. Biochem.* **266**, 26–32.
11. Tayyab, S., Siddiqui, M.U. & Ahmad, N. (1995) Experimental determination of the free energy of unfolding of proteins. *Biochemistry* **23**, 162–164.
12. Muzammil, S., Kumar, Y. & Tayyab, S. (2000) Anion-induced stabilization of human serum albumin prevents the formation of intermediate during urea denaturation. *Proteins: Struct. Funct. Genet.* **40**, 29–38.
13. Krishnakumar, S.S. & Panda, D. (2002) Spatial relationship between the prodan site, Trp-214, and Cys-34 residues in human serum albumin and loss of structure through incremental unfolding. *Biochemistry* **41**, 7443–7452.

14. Flora, K., Brennan, J.D., Baker, G.A., Doody, M.A. & Bright, F.V. (1998) Unfolding of acrylodan-labeled human serum albumin probed by steady-state and time-resolved fluorescence methods. *Biophys. J.* **75**, 1084–1096.
15. Baldwin, R.L. (1996) On-pathway versus off-pathway folding intermediates. *Fold. Des.* **1**, R1–R8.
16. Baldwin, R.L. (2001) Folding consensus? *Nat. Struct. Biol.* **8**, 92–94.
17. Kim, P.S. & Baldwin, R.L. (1982) Specific intermediates in the folding reactions of small proteins and the mechanism of protein folding. *Annu. Rev. Biochem.* **51**, 459–489.
18. Roder, H. & Colon, W. (1997) Kinetic role of early intermediates in protein folding. *Curr. Opin. Struct. Biol.* **7**, 15–28.
19. Sosnick, T.R., Mayne, L., Hiller, R. & Englander, S.W. (1994) The barriers in protein folding. *Nat. Struct. Biol.* **1**, 149–156.
20. Weissman, J.S. & Kim, P.S. (1992) Kinetic role of nonnative species in the folding of bovine pancreatic trypsin inhibitor. *Proc. Natl Acad. Sci. USA* **89**, 9900–9904.
21. Ptitsyn, O.B. (1995) Structures of folding intermediates. *Curr. Opin. Struct. Biol.* **5**, 74–78.
22. Creighton, T.E., Darby, N.J. & Kemmink, J. (1996) The roles of partly folded intermediates in protein folding. *FASEB J.* **10**, 110–118.
23. Privalov, P.L. (1996) Intermediate states in protein folding. *J. Mol. Biol.* **258**, 707–725.
24. Ferguson, N. & Fersht, A.R. (2003) Early events in protein folding. *Curr. Opin. Struct. Biol.* **13**, 75–81.
25. Daggett, V. & Fersht, A.R. (2003) Is there a unifying mechanism for protein folding. *Trends Biochem. Sci.* **28**, 18–25.
26. Levitt, M., Gerstein, M., Huang, E., Subbiah, S. & Tsai, J. (1997) Protein folding: the endgame. *Annu. Rev. Biochem.* **66**, 549–579.
27. Nolting, B. & Andert, K. (2000) Mechanism of protein folding. *Proteins* **41**, 288–298.
28. Tsong, T.Y. & Baldwin, R.L. (1972) Kinetic evidence for intermediate states in the unfolding of ribonuclease A. II. Kinetics of exposure to solvent of a specific dinitrophenyl group. *J. Mol. Biol.* **63**, 453–475.
29. Wetlaufer, D.B. (1973) Nucleation, rapid folding, and globular intrachain regions in proteins. *Proc. Natl Acad. Sci. USA* **70**, 697–701.
30. Chakraborty, S. & Peng, Z. (2000) Hierarchical unfolding of the alpha-lactalbumin molten globule: presence of a compact intermediate without a unique tertiary fold. *J. Mol. Biol.* **298**, 1–6.
31. Baldwin, R.L. & Rose, G.D. (1999) Is protein folding hierarchic? II. Folding intermediates and transition states. *Trends Briochem. Sci.* **24**, 77–83.
32. Baldwin, R.L. & Rose, G.D. (1999) Is protein folding hierarchic? I. Local structure and peptide folding. *Trends Briochem. Sci.* **24**, 26–33.
33. Kim, P.S. & Baldwin, R.L. (1990) Intermediates in the folding reactions of small proteins. *Annu. Rev. Biochem.* **59**, 631–660.
34. Santoro, M.M. & Bolen, D.W. (1988) Unfolding free energy changes determined by the linear extrapolation method. 1. Unfolding of phenylmethanesulfonyl alpha-chymotrypsin using different denaturants. *Biochemistry* **27**, 8063–8068.
35. Santra, M.K. & Panda, D. (2003) Detection of an intermediate during unfolding of bacterial cell division protein FtsZ: loss of functional properties precedes the global unfolding of FtsZ. *J. Biol. Chem.* **278**, 21336–21343.
36. Bhattacharyya, A., M. & Horowitz, P.M. (2001) The aggregation state of rhodanese during folding influences the ability of GroEL to assist reactivation. *J. Biol. Chem.* **276**, 28739–28743.
37. Chen, R.F. (1974) Fluorescence stopped-flow study of relaxation processes in the binding of bilirubin to serum albumins. *Arch. Biochem. Biophys.* **160**, 106–112.
38. Harmatz, D. & Blauer, G. (1975) Optical properties of bilirubin-serum albumin complexes in aqueous solution. A comparison among albumins from different species. *Arch. Biochem. Biophys.* **170**, 375–383.
39. Ogasahara, K. & Yutani, K. (1994) Unfolding-refolding kinetics of the tryptophan synthase alpha subunit by CD and fluorescence measurements. *J. Mol. Biol.* **236**, 1227–1240.
40. Sridevi, K., Juneja. J., Bhuyan, A.K., Krishnamoorthy, G. & Udgaonkar, J.B. (2000) The slow folding reaction of barstar: the core tryptophan region attains tight packing before substantial secondary and tertiary structure formation and final compaction of the polypeptide chain. *J. Mol. Biol.* **302**, 479–495.
41. Wallevik, K. (1973) Reversible denaturation of human serum albumin by pH, temperature, and guanidine hydrochloride followed by optical rotation. *J. Biol. Chem.* **248**, 2650–2655.
42. Wu, L.C., Peng, Z.Y. & Kim, P.S. (1995) Bipartite structure of the alpha-lactalbumin molten globule. *Nat. Struct. Biol.* **2**, 281–286.
43. Rischel, C., Thyberg, P., Rigler, F. & Poulsen, F.M. (1996) Time-resolved fluorescence studies of the molten globule state of apomyoglobin. *J. Mol. Biol.* **257**, 877–885.
44. Peng, Z.Y. & Kim, P.S. (1994) A protein dissection study of a molten globule. *Biochemistry* **33**, 2136–2141.